International Journal of Engineering Technology and Scientific Innovation

Volume:01,Issue:02

www.ijetsi.org

JET IMPINGING ON THE CYLINDRICAL BODY PLACED IN OPEN TUBE

V. I. Pinchukov

Siberian division of Russian Academy of Sc., In-te of Computational Technologies, Novosibirsk, 630090, Russia

ABSTRACT

Results of numerical search for new self-oscillatory compressible flows are presented. Two-dimensional Reynolds-averaged Navier-Stocks equations added by an algebraic turbulence model are solved by an implicit third order Runge-Kutta scheme. Interactions of supersonic jets with cylindrical bodies, placed in open tubes, are discovered to have self-oscillatory regimes. Search for unsteady flows is carried out at jet Mach numbers $1.1 \le M \le 1.2$.

Keywords: Self-Oscillatory Flows, Reynolds-Averaged Navier-Stocks Equations, High Resolution Methods, Runge-Kutta Schemes

INTRODUCTION

"Microscopic" oscillations exist in majority of compressible flows, particularly, in turbulent flows. These "microscopic" oscillations are transforming to "macroscopic" oscillations in some cases. To our opinion, there are next cases of this transformation possibility:

1. growth of oscillations for sufficiently long shear layers or long jets as a result of the Kelvin-Helmholtz instability (this growth is studied, for example, in [1-3]),

2. possibility of various locations of flow separation from the bluff body surface, which results moving of this points and formation of unsteady flows (see, for example, [4-6]),

3. resonance interactions resulted from the positive feedback effects.

This third case includes jet cavity interactions (see, for example, [7-9]), a jet impinging on a plate [10-15], open cavity flows [16-19], flows past snaked bodies [15, 20-22]. We suppose that self-oscillations of all these unsteady flows are resulted from resonance interactions of flow "active"

elements, namely, elements amplifying disturbances.

The supposition is used here that contact discontinuities and intersection points of shocks with shocks or shocks with contact discontinuities compose the flow set of "active" elements.

Possibility of the disturbances amplification by contact discontinuities is a result of the Kelvin-Helmholtz instability and is accepted. Inclusion of intersection points to a list of amplifiers [15,23] is made as a hypothesis, which is checked by results of a search for new unsteady flows.

We construct and investigate flows, containing "active" elements. Particularly, flows near blunted bodies (cylinders or cones), giving off opposite jets, were discovered to have unsteady regimes [23]. Here these investigations are continued. We study axis symmetrical flows near blunted cylinders, placed in open tubes. It occurred that most intensive self-oscillations are observed for jet Mach numbers closed to 1, so jet Mach numbers $1.1 \le M_{jet} \le 1.2$ are considered here. Systems of weak shocks may be contained in the region between the jet start and cylindrical body. It is clear that if the cylinder radius r_{cyl} is equal to the inner radius of tube r_{tub}, $r_{cyl}=r_{tub}$, Hartmann whistle is resulted. Similarly, if the cylinder radius r_{cyl} is sufficiently large, we have jet impinging on a plate. Since we want to find new self-oscillatory regimes, we use here jet radiuses which exceed cylinder radiuses and which are bounded by tube radiuses. We consider here only flows with ring jets moving near outward surfaces of the tube.

PHYSICAL AND COMPUTATIONAL MODELS

Reynolds-averaged Navier-Stocks equations added by an algebraic turbulence model are used here and in previous author's investigations [15,23]. A search for new self-oscillatory flows deals with trial calculations of numerous different flows. So, we need in a simple and universal turbulence model. Here the model is used, based on the Prandtl formulae

$$\mu=\rho|w|k^2z^2 \qquad (1)$$

where w is a vorticity, ρ is density, z is the length scale, k=0.4 is the von-Karman constant. This formulae is dealt in classical Cebeci-Smith and Baldween-Lomax models, where the length scale is defined as the recent point distance to the solid wall. Formulae (1) is used also in the Smagorinsky model of LES (Large Eddy Simulation), where the length scale is the grid cell size. Another definition is used here. We divide flows on vortex zones and ideal zones. The length scale is equal to zero in ideal zones and is equal to the recent point distance to the zone boundary in vortex zones, with next usage of the limitation written below.

The viscosity calculation starts with the determination of vortex zones by the velocity circulation calculation. The current

mesh cell belongs to any vortex zone if the inequality is true:

$$|w_{i+1/2,k+1/2}|S_{i+1/2,k+1/2} = |(u_{i+1/2,k}\Delta r_{i+1/2,k}) -$$
$$-(u_{i+1/2,k+1}\Delta r_{i+1/2,k+1}) + (u_{i+1,k+1/2}\Delta r_{i+1,k+1/2}) -$$
$$-(u_{i,k+1/2}\Delta r_{i,k+1/2})| > e\{|u_{i+1/2,k}||\Delta r_{i+1/2,k}| +$$
$$+|u_{i+1/2,k+1}||\Delta r_{i+1/2,k+1}| + |u_{i+1,k+1/2}||\Delta r_{i+1,k+1/2}| +$$
$$+|u_{i,k+1/2}||\Delta r_{i,k+1/2}|\},$$

where S is the mesh cell area, $\boldsymbol{u}$ are velocity vectors at mesh nodes, $\Delta\boldsymbol{r}$ are vectors connecting neighboring nodes, e is a small constant (for which the value $3/N$ is chosen in trial calculations, N - the most number of mesh points in space variables), $(\boldsymbol{u}\Delta\boldsymbol{r})$ are scalar multiplications of vectors, $|\boldsymbol{u}||\Delta\boldsymbol{r}|$ are multiplications of vector lengths. The middle part of this relation represents approximately the velocity circulation along mesh cell boundaries. The length scale z is calculated by formulas:

$z=d[x-(x/1.5)^3/2]$, if $x=L/d < 1.5$, $z=d$, if $x>1.5$.

where L – the recent point distance to the vortex zone boundary, d – a delimiting parameter. These formulas define a delimiter with continuous first derivative. Calculations, presented here, are carried out for $d=r_{tub}/60$, r_{tub} – the tube inner radius.

The used here approach deals with the fixed aggregate of scales of disturbances represented in the turbulent viscosity. As a result, the turbulent viscosity is steady while the mesh number is varying and, consequently, the contact discontinuities thickness (more precisely, shift layers in our case) is steady while the mesh number is varying. It makes possible checking of the solutions convergence in the mesh nodes number and, consequently, makes possible additional verification of the unsteady regimes existence.

An implicit conservative Runge-Kutta scheme [24] is employed here with some modifications. Initial method [24] is implemented in a computer code for sufficiently smooth curvilinear coordinate transformations $x=x(a,b)$, $y=y(a,b)$, mapping the unit square in the plane of variables a,b to a curvilinear quadrangle in the plane of physical variables x, y. Within this approach, it is difficult to obtain satisfactory meshes for complicated physical domains. For that reason, a special version of the code is developed for the case when functions $x=x(a,b)$, $y=y(a,b)$ perform mapping of the unit square with excisions $\{0\le a\le a_0, 0\le b\le b_0\}$, $\{a_1\le a\le 1, 0\le b\le b_1\}$ to a curvilinear quadrangle with curvilinear quadrangular excisions (see **fig**. 1). This version allows carrying out calculations, described below, without dividing complicated domains into sub-domains. Both recent method and method [24] are third order in time and fourth order in space (viscous terms are approximated with second order).

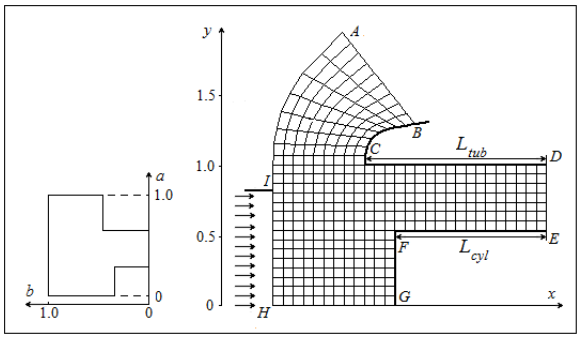

Figure 1. Schematic representation of a domain, a mesh and a jet.

Figure 1 represents schematically a flow near a cylindrical body, placed in an open tube. There is a uniform supersonic jet, out flowing from a nozzle at the left side of the picture. All variables are prescribed at inflow boundaries (*HI,IA*). The tangential velocity component is equal to zero and other variables are extrapolated at solid surfaces (*CB,CD,FE,FG*), which are represented in **fig**. 1 by bold lines. The radial velocity component is equal to zero at the symmetry axis, other variables are extrapolated. Extrapolation conditions are used at the tube exit (*DE*). The upper boundary (AB) requires complicated conditions. Extrapolation conditions are used at this boundary as a rule. In some cases the velocity component, normal to this boundary, becomes negative, which leads to instability of the numerical solution. To avoid this instability we prescribe zero value of this component at the boundary and in the vicinity of the boundary. Test calculations show, that numerical results are not sensitive to variation of this boundary place, if this boundary is sufficiently distant.

Naturally, numerical calculations deal with dimensionless variables. These variables are defined as relations of initial variables and next parameters of the outer stream or the body size: p_∞ - for pressure, ρ_∞ - for a density, $\sqrt{p_\infty/\rho_\infty}$ - for a velocity, r_{tub} (the inner tube radius) – for space variables, $r_{tub}/\sqrt{p_\infty/\rho_\infty}$ - for time.

An open cavity flow [17,18] and an under expanded supersonic jet impinging on a plane [14] are were used for comparison to verify the numerical method and the turbulence model.

This cavity flow is tested numerically with flow field condition M_∞=2, the cavity depth – length ratio is 0.5. The time history of the surface pressure at the x=2L/3 point on the cavity floor is used to form the time averaged sound pressure level $\overline{SPL}$, which is computed by the equation

$$\overline{SPL}=20\ \mathrm{Log}_{10}\ (\Delta p\ /p_{ref}),\ p_{ref}=20\mathrm{mkPa}/p_\infty, \qquad (2)$$

where

$$\Delta p=\sqrt{\overline{p'^2}},\qquad \overline{p'^2}=\sum_n (p_n-\overline{p})^2/N, \qquad (3)$$

.

p_∞=98066Pa (air pressure under normal conditions) is used since dimensionless variables are dealt here. The resulting time averaged $\overline{SPL}$ of 174.8Db may be compared with the numerical $\overline{SPL}$ of

167.54Db and the experimental $\overline{SPL}$ of 164.41Db resulted in [17]. The weighted $\overline{SPL}$ for data from various sources [18] is approximately 171Db.

Jet impinging on a plate [14] is computed [15] with flow field conditions M_{jet}=2.098 (Mach number at the exit cross section of the nozzle), p_{jet}/p_{∞}=4.785, γ=1.4, h_{jet} =6.95r_{jet} (h_{jet} – the nozzle exit distance to the plate, r_{jet} - the nozzle radius), σ_{jet}=4° (the nozzle half-angle). The 696×463 mesh is used. The resulting frequency of 8206Hz may be compared with the experimental frequency of 9033Hz , presented in [14].

RESULTS AND DISCUSSION

Figure 2 shows the density distribution, calculated for flow conditions M_{jet}=1.1, ρ_{jet}=0.25 (in dimensionless form), p_{jet}=0.7. Geometry parameters are r_{cyl}=0.6, r_{jet} =0.8, h_{jet}=1.3 (the distance of the nozzle exit section to the cylinder surface), L_{tub}=1.0, L_{cyl}=1.3, (L_{tub} and L_{cyl} - tube and cylinder lengths). The 575×586 mesh is used, excisions contains 168×325 and 180×390 points.

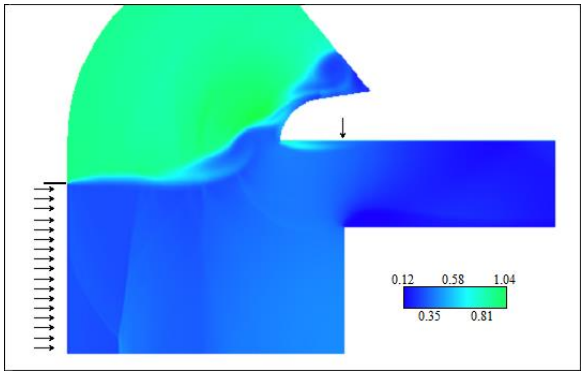

Figure 2. The density distribution, M_{jet} =1.1.

There is jet near outward surfaces of the tube. Weak shock waves compose “lambda” configuration near axe y=0.

Intensive self-oscillations exist in this flow. It may be seen in **fig**. 3, where density histories are shown for the point, signed by an arrow in **fig**. 2. Calculations are carried out for the 515x586 mesh (the 23-56 time interval) and for the 762x883 mesh (the 39.5-56 time interval). Initial flow fields for the last mesh are obtained by linear interpolation of discrete solution from the 515x586 mesh.

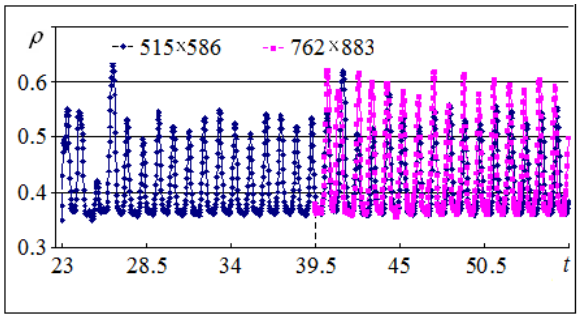

Figure 3. Density histories for the inner surface of the tube

The calculations accuracy may be evaluated on the base of density histories shown in fig.3. Discrete solution for the 515x586 mesh produces lesser oscillations then solution for the 763x883 mesh. It may be explained by the greater influence of numerical dissipation for meshes with lesser number of points. Fig. 4 shows the density distribution for the 763x883 mesh. Density fields shown in figs. 3 and 4 corresponds to the same time moment t=56. Comparison of these **figs**. gives additional evaluation of the computations accuracy.

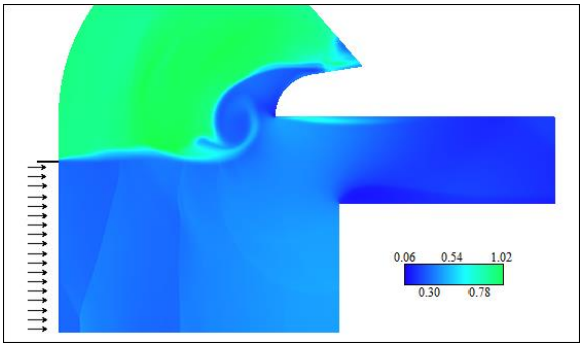

Figure 4. The density distribution, the 763x883 mesh.

Density histories represented in fig. 3 show nearly periodical behavior with the T=0.95 period. Flow fields dynamics for the [56.0, 56.0+T] time interval is shown in figs. 4-8, which correspond to time moments t=56.0, t=56.0+T/4, t=56.0+T/2, t=56.0+3T/4, t=56.0+T. The 763x883 mesh is used.

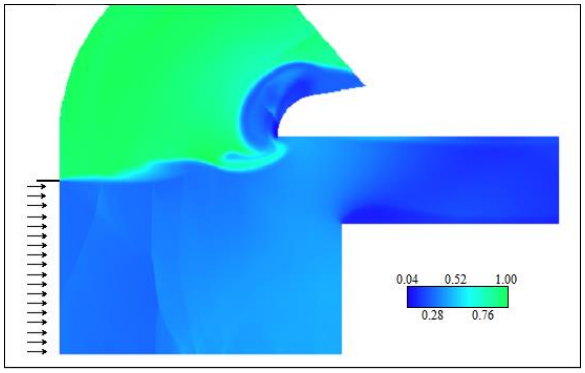

Figure 5. The density distribution, t=56.0+T/4

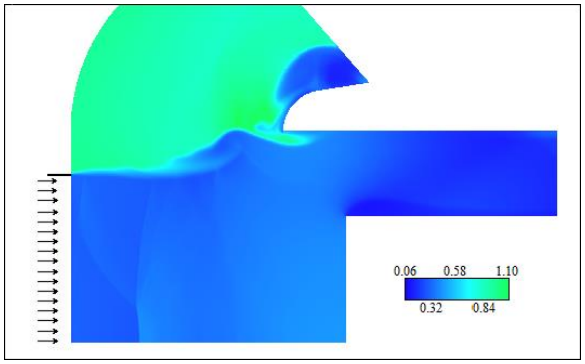

Figure 6. The density distribution, t=56.0+T/2

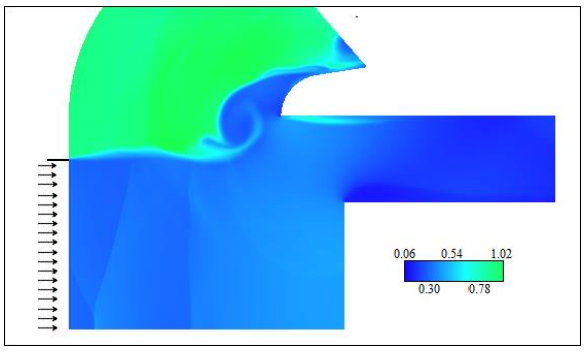

Figure 7. The density distribution, t=56.0+3T/4.

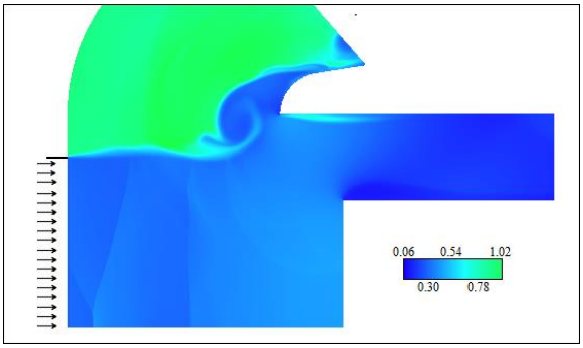

Figure 8. The density distribution, t=56.0+T.

Density distributions, shown in figs. 4 and 8, correspond to time moments differing by one period, so these distributions are alike. The unique feature of the considered solution is a discontinued character of the jet, moving along the outward surface of the tube. Next ideas may be suggested to explain this character. Shock waves which appear in flows with Mach numbers closed to 1 are highly sensitive to any disturbances. Different patterns of weak shock waves are seen in figs 4-8. The change of the shock waves pattern disturbs the outer flow, especially this change disturbs the jet boundary as a result of the Kelvin-Helmgoltce instability. This disturbed flow influences on shock waves. So conditions are formed for the positive feedback effect. As a result, a resonance may take place, which induces self-oscillations of the flow. These self-oscillations are sufficiently intensive to provide a discontinued character of the jet, moving along the outward surface of the tube.

It should be noted that the possibility of a resonance, leading to oscillations appearing, depends on the flow structure. We cannot predict these resonance possibility and oscillations appearing. For example, the flow, considered below, contains two shocks in the jet start region. But this flow is steady.

Figure 9 shows the density distribution, calculated for flow conditions $M_{jet}=1.2$, $\rho_{jet}=0.25$, $p_{jet}=0.7$. Geometry parameters are $r_{cyl}=0.6$, $r_{jet}=0.8$, $h_{jet}=1.5$ (the distance of the nozzle exit section to the cylinder surface), $L_{tub}=1.0$, $L_{cyl}=1.3$, (L_{tub} and L_{cyl} - tube and cylinder lengths). The 575×586 mesh is used.

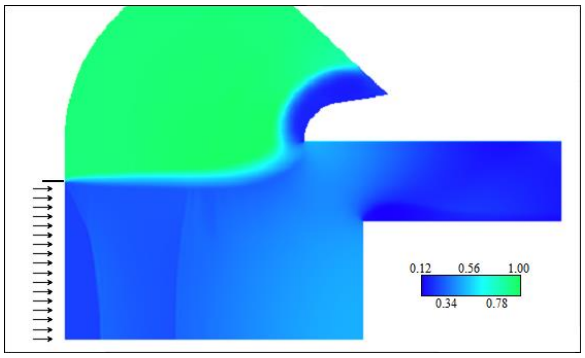

Figure 9. The density distribution, $M_{jet}=1.2$.

CONCLUSION

Numerical search for new self-oscillatory compressible flows, started in [15,23], is continued in recent paper. Supersonic jet impinging on cylindrical bodies, placed in

open tubes, is investigated at jet Mach numbers closed to 1. The unique feature of one of the considered flows is a discontinued character of the jet, moving along the outward surface of the tube. We suppose that the self-oscillatory mechanism of these flows bases on resonance interaction of two "active" elements, namely, systems of weak shocks, placed between the jet start and cylindrical body, which are highly sensitive to flow disturbances in the case of flow Mach number closed to 1, and jet boundaries, amplifying disturbances as a result of the Kelvin-Helmgoltce instability.

Nomenclatures

p_{jet} - jet pressure,

ρ_{jet} - jet density,

M_{jet} - jet Mach number,

μ - viscousity,

w - vorticity,

z - length scale,

γ - specific heat ratio,

r_{cyl} - cylinder radius,

r_{jet} - jet radius,

r_{tub} - tube radius,

h_{jet} - distance of nozzle exit section to cylinder surface,

L_{cyl} - cylinder length,

L_{tub} - tube length

REFERENCES

[1] Berland J., Bogey C., Bailly C. Numerical Study of Screech Generation in a Planar Supersonic Jet, Phys. Fluids, Vol. 19, 2007, 75-105.

[2] Georgiadis N., Alexander J., Reshotko E. Hybrid Reynolds-Averaraged Navier-Stokes/Large-Eddy Simulation of Supersonic Turbulent Mixing, AIAA Journal, V. 41, N. 2, 2003, 218-229.

[3] Berland J., Bogey C., Bailly C. Large Eddy Simulation of Screech Tone Generation in a Planar Under expanded Jet, 12th AIAA/CEAS Aeroacoustics Conference, 2006, 8-10.

[4] Perry A. E., Chong M. S. and Lim T. The vortex-shedding process behind two-dimensional bluff bodies, Journal of Fluid Mechanics 116, 1982, 77-90.

[5] Roshko A. Perspectives on bluff body aerodynamics, Journal of Wind Engineering and Industrial Aerodynamics 49, 1993, 79-100.

[6] Taylor Z.J., Palombi E., Gurka R. & Kopp G.A. Features of the turbulent flow around symmetric elongated bluff bodies, J. Fluids Struct., 27, 2011, 250-265

[7] Raman G., Envia E., Bencic T. J. Jet Cavity Interaction Tones, American Institute of Aeronautics and Astronautics J., Vol. 40 (8), 2002, 1503–1511.

[8] Murugappan S., Gutmark E. Parametric Study of the Hartmann–Sprenger Tube, Experiments in Fluids, Vol. 38 (6), 2005, 813–823.

[9] Kastner J., Samimy M. Development and Characterization of Hartmann Tube Fluid Actuators for High-speed Control, American Institute of Aeronautics and Astronautics J., Vol. 40 (10), 2002, 1926–1934.

[10] Henderson B., Bridges J., Wernet, M. An Experimental Study of the Oscillatory Flow Structure of Tone-Producing Supersonic Impinging Jets, J. Fluid Mech., Vol. 542, 2005, 115–137.

[11] Kuo C.-Y., Dowling A. P. Oscillations of a Moderately Under expanded Choked Jet Impinging Upon a Flat Plate, J. Fluid Mech., Vol. 315, 1996, 267–291.

[12] Sakakibara Y., Iwamoto J. Numerical Study of Oscillation Mechanism in Under expanded Jet Impinging on Plate, J. Fluids Eng. , Vol. 120, 1998, 477.

[13] Gorshkov G. F., Uskov V. N. Specialties of Self- Oscillations, Arising from Interaction of Supersonic Under expanded Jet with Finite Obstacle, Prikl. Mekh. Tekh. Fiz., 40(4), 1999, 143-149 (in Russian).

[14] Adrianov A. L., Bezrukov A. A., Gaponenko Yu. A. Numerical Study of Interaction of a Supersonic Gas Jet with a Flat Obstacle. Prikl. Mekh. Tekh. Fiz., 41(4), 2000, 106-111 (in Russian).

[15] Pinchukov V. I. Numerical Modeling of Non-Stationary Flows with Transient Regimes, Comput. Mathem. and Mathem. Physics, Vol. 49 (10), 2009, 1844–1852.

[16] Rossiter J. Wind-Tunnel Experiments on the Flow over Rectangular Cavities at Subsonic and Transonic Speeds. Technical Report Reports & Memoranda 3438, Aeronautical Research Council, 1964.

[17] Tam C.-J., Orkwis P.D., Disimile P.J. Comparison of Baldwin-Lomax Turbulence Models for Two-Dimensional Open-Cavity Calculations, AIAA J., Vol. 34(3), Technical Notes , 1996, 629- 632.

[18] Tam C.-J., Orkwis P.D., Disimile P.J. Algebraic Turbulence Model Simulations of Supersonic Open-Cavity Flow Physics, AIAA J., Vol. 34(11), 1996, 2255-2260.

[19] Murray N, Sällström E., and Ukeiley L., Properties of subsonic open cavity flow fields, Physics of Fluids, vol. 21, pp. 095103-16, 2009.

[20] Gauer M., Paull A., Numerical investigation of a Spiked Nose Cone at Supersonic Speeds, Journal of Spacecraft and Rockets, V.45, N. 3, 2008, 459-471

[21] Caarese W. and Hankey W. L. Modes of Shock Wave Oscillations on Spike

Tipped Bodies, AIAA Journal, Vol. 23, No.2, 1985, pp: 185-192

[22] Mehta R.C. Pressure Oscillations Over a Spiked Blunt Body at Hypersonic Mach Number, Computational Fluid Dynamics Journal, Vol.9, No.2, July 2000, pp. 88-95.

[23] Pinchukov V. I. Modeling of Self-Oscillations and a Search for New Self-Oscillatory Flows, Mathematical Models and Computer Simulations, Vol. 4(2), 2012, 170–178.

Pinchukov V. I. Numerical Solution of the Equations of Viscous Gas by an Implicit Third Order Runge-Kutta Scheme, Comput. Mathem. and Mathem. Physics, Vol. 42(6), 2002, 898-907.